924 *Biochemistry* **2010,** *49,* 924–933
DOI: 10.1021/bi901811s

BIOCHEMISTRY
including biophysical chemistry & molecular biology
Article

Biophysical Properties of the Eukaryotic Ribosomal Stalk[†]

Przemysław Grela,[‡,⊥] Dawid Krokowski,[‡,⊥] Yuliya Gordiyenko,[§] Daniel Krowarsch,[∥] Carol V. Robinson,[§] Jacek Otlewski,[∥] Nikodem Grankowski,[‡] and Marek Tchórzewski*[,‡]

[‡]*Department of Molecular Biology, Maria Curie-Skłodowska University, Akademicka 19, 20-033 Lublin, Poland,* [§]*Department of Chemistry, University of Cambridge, Lensfield Road, Cambridge CB21EW, United Kingdom, and* [∥]*Laboratory of Protein Engineering, University of Wroclaw, Tamka 2, 50-137 Wroclaw, Poland.* [⊥]*These two authors contributed equally.*

Received October 22, 2009; Revised Manuscript Received January 8, 2010

ABSTRACT: The landing platform for the translational GTPases is located on the 60S ribosomal subunit and is referred to as a GTPase-associated center. The most distinctive feature of this center is an oligomeric complex, the stalk, responsible for the recruitment of translation factors and stimulation of translation factor-dependent GTP hydrolysis. In eukaryotes, the stalk has been investigated *in vitro* and *in vivo*, but most information available concerns its individual components only. In the present study, we provide an insight into the biophysical nature of the native stalk isolated from the yeast *Saccharomyces cerevisiae*. Using fluorescence, circular dichroism, and mass spectrometry analyses, we were able to characterize the natively formed yeast stalk, casting new light on the oligomeric properties of the complex and its quaternary topology, showing that folding and assembly are coupled processes. The pentameric stalk is an exceptionally stable structure with the protein core composed of P0, P1A, and P2B proteins and less tightly bound P1B and P2A capable of dissociating from the stalk core. We obtained also the whole picture of the posttranslational modifications at the logarithmic phase of yeast growth, using mass spectrometry approach, where P proteins are phosphorylated at a single serine residue, P0 may accept two phosphate groups, and P1A none. Additionally, only P1B undergoes N-terminal acetylation after prior methionine removal.

All major steps of protein synthesis, i.e., initiation, elongation, and termination, are dependent on translational GTPases (tGTPases) which promote transitions between different functional/structural states of the ribosome (*1*). The binding site for the tGTPases is referred to as a factor-binding region or a GTPase-associated center (GAC) in conjunction with the sarcin−ricin loop (SRL) and is located on the 60S ribosomal subunit (*2*, *3*). The most prominent structure recognized in the GAC is called the stalk (*4*−*6*). The common functional denominator of the ribosomal stalks from all domains of life is recruitment of tGTPases and stimulation of factor-dependent GTP hydrolysis during translation (*3*). A unique characteristic of the stalk is that its activity depends mainly on ribosomal proteins (r-proteins), unlike other ribosomal processes which are, in general, RNA-dependent (*7*). The protein part of this region comprises two components. The first one, in prokaryotes/eukaryotes, is represented by the L11/L12 protein which is attached to the main body of the 60S via helices 43/44 of 28S rRNA and is referred to as a molecular switch (*8*). It forms a part of the stalk base (*9*). The second component of the stalk is an oligomeric complex with a composition dependent on the taxonomic position of the organism. In prokaryotes, this complex occurs in two structural configurations. Pentameric complex L10-$(L12)_4$ is found in mesophiles, while heptameric organization L10-$(L12)_6$ has been reported for thermophiles (*3*, *10*). A similar diversity was found in archaeal/eukaryotic ribosomes, where a heptamer L10-$(L12)_6$ was observed in archaea (*11*), and pentamer P0-$(P1\text{-}P2)_2$ in eukaryotes (*12*). The L10/P0 protein forms the base of the stalk and anchors the complex to the 60S subunit (*5*). Interestingly, in eukaryotes there is a further diversification among the P proteins. The P0 protein, the orthologue of bacterial L10, has two independent domains. The first one, the rRNA binding domain, can be exchanged with its bacterial counterpart (*13*), while the second one, the P domain, has an extension of the polypeptide unique to eukaryotes (*14*). This distinctive sequence is responsible for anchoring the P1/P2 proteins and for specific interactions with eukaryotic elongation factors (*15*). The P1/P2 polypeptides are regarded as analogous to bacterial L12 (*Escherichia coli* L7/L12), because there is a clear functional link but no structural similarity or evolutionary relations (*16*). Furthermore, in lower eukaryotes, e.g., *Saccharomyces cerevisiae*, the P1/P2 proteins have undergone further structural expansion into four polypeptides, P1A, P1B, P2A, and P2B. The P proteins are responsible not only for stimulation of GTP hydrolysis but also for factor binding specificity toward eukaryotic translation factors (*13*). Additionally, the P1/P2 proteins are not absolutely required for cell viability, in contrast to the bacterial L12 protein (*17*), while the P0 protein is an essential stalk element and can compensate for a lack of P1/P2 proteins (*18*). However, the whole pentameric complex is indispensible for optimal ribosomal activity and cell survival (*19*). The structural and biochemical information about the eukaryotic stalk as a whole is scarce, and only a plethora of *in vitro* and *in vivo* analyses of individual stalk components have been reported. These *in vitro* and *in vivo* studies have brought considerable insights into the molecular anatomy of the eukaryotic stalk, showing that the P1/P2 proteins form stable, functionally relevant heterodimers (*20*−*26*), with the P1 proteins anchoring the dimers (*22*, *23*) at two independent interaction sites

[†]This work was partially supported by Grant N302 061034 from the Ministry of Science and Higher Education.

*Corresponding author. Telephone: +48-81-537 59 56. Fax: +48-81-537 59 07. E-mail: maro@hektor.umcs.lublin.pl.

 Published on Web 01/08/2010

on the P0 protein (*19*, *27*). The mode of assembly of the stalk has also been approached, demonstrating functional distinction between the two P1/P2 dimers (*28*). Additional analysis showed that P1 proteins are in close proximity to P0, and P2 might be exposed to the solvent (*12*). However, despite that scattered information, the stalk as a whole has never been subjected to analysis because of its complex protein composition and a tedious *in vitro* procedure used for its isolation.

To overcome the latter obstacle, we have developed a novel procedure to isolate the stalk from a genetically engineered strain of the yeast *S. cerevisiae*. The procedure allowed us to isolate for the first time a natively assembled pentameric complex, as well as its truncated form. Using several biophysical methods, we were able to provide the first insight into the biochemical behavior of the whole functional part of the stalk. Additionally, we provide the first view of the posttranslational modifications of the stalk as a whole structure at a logarithmic phase of cell growth. Finally, the obtained data allowed us to propose the mode of assembly of the stalk which might explain the exchangeability of the P proteins observed earlier.

MATERIALS AND METHODS

Sample Preparation. The preparation of the yeast 80S ribosome particles and protein complexes was done as described previously (*19*), using the yeast mutants P0TH199 (*MAT**a**; RPP0-TH199; his3*Δ*1; leu2*Δ*0; lys2*Δ*0; ura3*Δ*0*) and P0TH230 (*MAT**a**; RPP0-TH230; his3*Δ*1; leu2*Δ*0; lys2*Δ*0; ura3*Δ*0*) where a short amino acid sequence recognized by thrombin was introduced into the P0 protein at positions 199 and 230. Briefly, 80S ribosomal particles from P0TH199 or P0TH230 yeast cells were incubated with activated thrombin from bovine plasma (Sigma) for 12 h at 4 °C (10 mg of 80S/1 unit of thrombin) to release pentameric or trimeric complexes. Then ribosomal particles were removed by centrifugation at 105000*g* for 2 h. The obtained supernatant fraction was used as a source of P protein complexes, which were subsequently purified with Ni-NTA agarose and size-exclusion chromatography using the Akta Purifier FPLC system from GE Healthcare Life Sciences, equipped with the Superose 12 HR 10/30 gel filtration column. The purity of the obtained P protein complexes was verified by 14% SDS−PAGE[1] and 10% native PAGE according to Laemmli's method. Protein concentration was measured according to Bradford's method using a Bio-Rad protein assay kit or basing on the absorbance at 280 nm using an extinction coefficient calculated from the amino acid composition of the TH199 and TH230 complexes according to the method described previously (*29*).

Spectroscopic Analyses. All measurements were carried out in 10 mM Tris-HCl (pH 7.4), 10 mM $MgCl_2$, 150 mM NaCl, and 5 mM β-mercaptoethanol, at protein concentrations between 1 and 5 μg/mL. Fluorescence spectra were recorded on an FP-750 spectrofluorometer (Jasco) equipped with a Peltier accessory ETC 272T. An excitation wavelength of 280 nm was used, and emission spectra were collected from 310 to 420 nm in a 10 mm cuvette with 5 nm emission and excitation bandwidths at 21 °C. Thermal denaturation was studied using circular dichroism (CD) and fluorescence (FL). CD experiments were carried out with a Jasco J-715 spectropolarimeter equipped with a Peltier accessory PFD 350S. The temperature-induced ellipticity changes at 222 nm were followed using a slit width of 2 nm and 4 s response time in a 4 mm cuvette. Fluorescence measurements monitoring changes in the emission signal at 350 nm on excitation at 280 nm, with 5 nm emission and excitation bandwidths, were performed using an FP-750 spectrofluorometer. The automatic Peltier accessory allowed continuous monitoring of the thermal transition at a constant rate of 1 deg min^{-1} and 1 °C min^{-1}. Using the PeakFit software (Jandel Scientific Software), the plots of spectroscopic signals versus temperature were fitted to a two-state denaturation model. Chemical unfolding of protein samples was performed in various concentrations of urea or guanidine hydrochloride (Gdn-HCl) in 10 mM Tris-HCl, pH 7.5; samples were equilibrated for at least 12 h at 21 °C. The transitions were monitored by the decrease of the CD signal at 222 nm with a 2 nm bandwidth or by the decrease of intrinsic fluorescence at 350 nm on excitation at 280 nm with 5 nm emission and excitation bandwidths. The apparent free energy change in the absence of Gdn-HCl (ΔG_{H_2O}) was determined by fitting the ellipticity or fluorescence intensity changes at particular concentrations of Gdn-HCl to the equation derived by Santoro and Bolen (*30*).

Mass Spectrometry. All complexes were analyzed by using a modified Q-ToF 2 mass spectrometer (Waters, Manchester, U.K.) described in ref *31*. For the analysis, protein solutions were buffer exchanged into 200 mM ammonium acetate (pH 7.5) using Micro Bio-Spin chromatography columns (Bio-Rad). To assess the stability of the ribosomal stalk complexes, ethanol and DMSO were used as chaotropic agents. After exchange into ammonium acetate, ethanol or DMSO was added to the final concentration as indicated, and the complexes were incubated for 15 min before being subjected to mass spectrometry analysis. Aliquots of ~2 μL were introduced into the mass spectrometer via nanoflow capillaries, and the conditions used for solution disruption experiments were as follows: capillary voltage 1.2 kV, extractor voltage 2 V, collision voltage 4 V, and cone voltage 80 V. For cone ramp experiments the following conditions were used: capillary voltage 1.2 kV, extractor voltage 2 V, collision voltage 4 V, and cone voltage in the range 80−180 V. For collision experiments: capillary voltage 1.2 kV, extractor voltage 2 V, cone voltage 80 V, and accelerating voltage was varied at 4−160 V at an argon pressure of 3.0×10^{-2} mbar in the collision cell to study in-cell CID. Pressure at the ion transfer stage was maintained at 9.3×10^{-3} mbar. The pressure at the front end of the instrument was adjusted for optimal signal.

RESULTS

Spectroscopic Studies. So far, the majority of our knowledge about the biological behavior of the stalk structure comes from integration of scattered data, because no systematic studies of the native stalk have been undertaken until now. To stop this gap, we isolated the native stalk from previously obtained yeast mutant strains P0TH199 and P0TH230 (*19*). Two complexes were obtained. The first one, the pentameric complex TH199, contains a truncated P0 protein with the rRNA binding domain removed, and only the P domain left intact, comprising amino acids 199−312 able to bind the P1A-P2B and P1B-P2A dimers, and is described as $\Delta P0_{199-312}$-(P1A-P2B)-(P1B-P2A). The second complex, TH230, is a further deletion form of TH199 containing a trimmed variant of P0 (amino acids 230−312) able to bind only one dimer, P1B-P2A. Therefore, TH230 is a trimer, $\Delta P0_{230-312}$-(P1B-P2A). The complexes were purified to homogeneity using affinity chromatography and size-exclusion chromatography, following an earlier developed procedure (*19*) (Figure 1). As a first approach for biophysical characterization of the two complexes, we analyzed their intrinsic fluorescence

Table 1: Thermodynamic Parameters for Chemical and Thermal Denaturation of TH199 and TH230 Complexes[a]

	ΔG_{H_2O}[a] (kcal mol^{-1})	Gdn-HCl$_{1/2}$[a] (M)	$-m$[a] (kcal mol^{-1} M^{-1})	ΔG_{H_2O}[b] (kcal mol^{-1})	Gdn-HCl$_{1/2}$[b] (M)	m[b] (kcal mol^{-1} M^{-1})	T_m[c] (°C)	ΔH_{den}[c] (kcal mol^{-1})	T_m[d] (°C)	ΔH_{den}[d] (kcal mol^{-1})
TH199	7.23	2.60	2.78	7.27	2.58	2.81	67.5	111	65.7	118
TH230	3.24	1.41	2.30	3.14	1.40	2.27	56.9	54.4	56.4	58.8

[a]Uncertainties in ΔG_{den} are about 0.2 kcal/mol, in ΔH_{den} 5 kcal/mol, and in T_m 0.2 °C. Gdn-HCl-induced unfolding monitored by changes of ellipticity. [b]Gdn-HCl-induced unfolding monitored by changes of fluorescence. [c]Thermal-induced unfolding monitored by changes of ellipticity. [d]Thermal-induced unfolding monitored by changes of fluorescence.

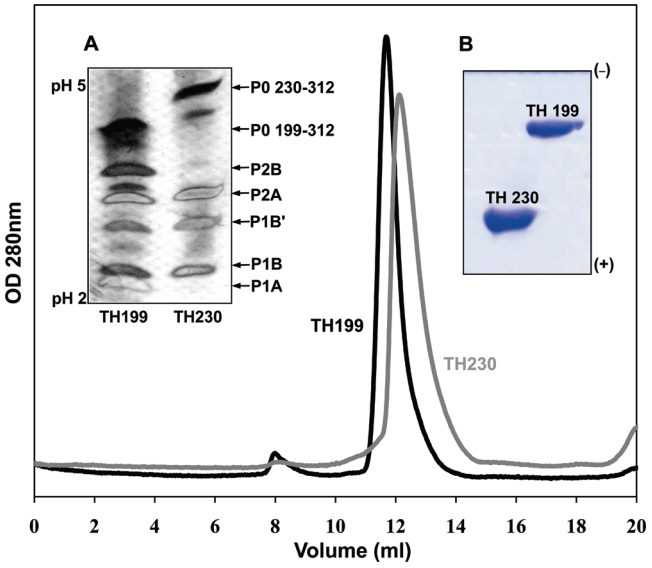

FIGURE 1: Purification of pentameric (TH199) and trimeric (TH230) complexes. Purified complexes were subjected to analytical size-exclusion chromatography. (A) Protein fractions from protein peaks were analyzed by isoelectrofocusing. Individual P proteins are marked by arrows. P1B′ describes proteolytically N-terminaly cleaved P1B protein. (B) Native PAGE of pentameric and trimeric complexes stained with Coomassie brilliant blue R-250; 10 μg of protein was loaded.

properties recognized as a very sensitive probe of the tertiary structure characteristics. The fluorescence spectrum of tyrosine and tryptophan residues (excitation at 280 nm) of TH199 at various pH values showed a maximum centered at 337 nm (Figure 2A), while that for TH230 exhibited the maximum at 349 nm (Figure 2B). The emission spectra were almost identical at all the pH values tested except at pH 2, where the maximum was blue shifted toward 333 nm in both cases, indicating that the complexes underwent aggregation. An intriguing observation was made when 8 M urea used as a denaturant. At an alkaline pH (7.5 and 9.0) the TH199 complex was resistant to urea treatment, but altering pH toward more acidic values, pH 6.8 and especially pH 5.0, it resulted in unfolding of the complex, where the maximum was red shifted toward 350 and 355 nm, respectively (Figure 2C). On the other hand, TH230 unfolded easily in the whole range of pH, exhibiting a new fluorescence maximum at 355 nm, diagnostic of a tryptophan indole group fully exposed to the solvent (Figure 2D). In order to evaluate the structural stability of the TH199 and TH230 complexes further, their unfolding was studied as a function of urea concentration. The resulting conformational transitions were monitored as changes of fluorescence intensity at 350 nm against urea concentration. The TH199 complex showed considerable stability in the whole range of urea concentrations (Figure 2E). In contrast, the denaturation of the TH230 complex was fully cooperative, following closely a two-state transition mechanism (Figure 2E). Since 8 M urea did not exert a significant effect on the TH199 complex, a stronger denaturant, guanidine hydrochloride (Gdn-HCl), was used for the subsequent unfolding experiment. The stability of the complexes was analyzed with the aid of two methods, far-UV CD, which usually follows secondary structure perturbations, and fluorescence spectroscopy, which is sensitive to tertiary/quaternary structural changes. The fluorescence- and CD-monitored Gdn-HCl denaturation curves of the complexes were acquired at pH 7.5. The reversibility of the Gdn-HCl-induced unfolding was >90%, and the results were independent of protein concentration (data not shown). For both complexes the denaturation curves showed a fully cooperative unfolding behavior, and the results obtained by fluorescence and CD agreed well and were consistent with a two-state model for unfolding (Figure 3A). In accord with the urea unfolding, remarkable differences in the stability of the two complexes were observed also in the case of Gdn-HCl-induced denaturation. The thermodynamic parameters calculated for the two complexes (Table 1) indicated that TH199 is almost twice as stable as the TH230 complex. In addition, the stability of the complexes was analyzed as a function of temperature using CD and fluorescence measurements. Large differences in stability were also observed, with transition midpoints at 65 or 67 °C for TH199 and 56 °C for TH230 (Figure 3B and Table 1). Thus, all of these spectroscopic data illustrate that the TH199 complex displays much higher chemical and thermal stability than does TH230. Nevertheless, for both complexes a two-state transition mechanism may be assumed, indicating that there are no detectable folding intermediates upon unfolding of the complexes during chemical or thermal denaturation.

Mass Spectrometry Analysis of the Native Stalk Complex. Having accomplished the spectroscopic studies which showed an unusual stability of the pentameric complex, we have applied a nondenaturing mass spectrometry approach to study protein−protein interactions of the noncovalent protein complexes. This technology constitutes a bridge between traditional biochemical/biophysical methods and structural X-ray analysis or cryoelectron microscopy and is a novel structural biology approach to study "functional modules" in various biological complexes (*32*, *33*), even in the megadalton range. Initially, to probe the stability of the TH199 and TH230 ribosomal stalk complexes, we used both in-cell and in-source collision-induced dissociation to analyze the behavior of the complexes in the gas phase. As a first approach, we used stepwise increasing accelerating voltages (20−100 V) in the collision cell. As shown in Figure 4, at a low accelerating voltage (20 V) the complexes were stable in the gas phase and were seen as a set of peaks with different charge states (TH199 from 13+ to 16+; TH230 from 10+ to 12+, marked by box), with masses of 56763 and 31393 Da for the pentamer and trimer, respectively. With increasing voltage individual P proteins started to dissociate from the complexes,

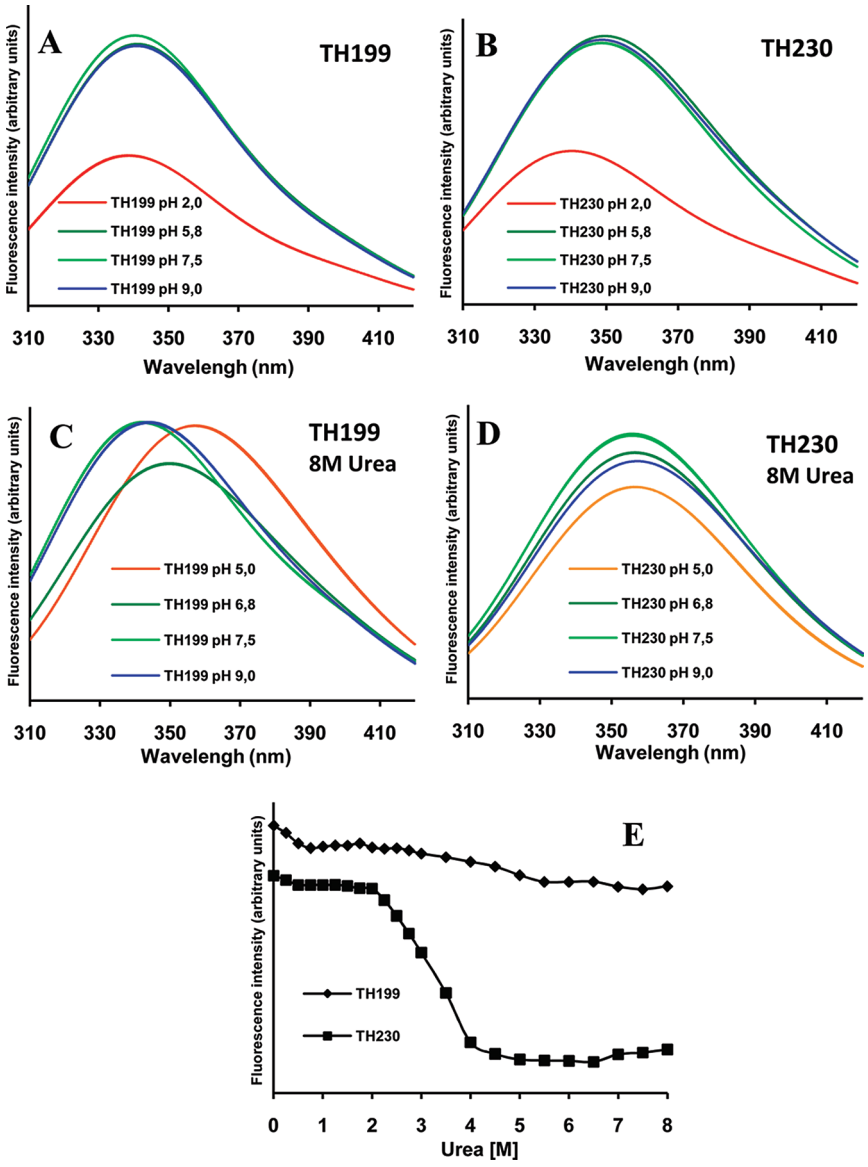

FIGURE 2: Intrinsic fluorescence properties of pentameric (TH199) and trimeric (TH230) stalk complexes. (A, B) Influence of pH on complex stability. For alkaline pH, 10 mM Tris-HCl buffer was used. For acidic pH 2, glycine buffer was applied, and pH 5 was adjusted with acetate buffer. All buffers were supplemented with 10 mM $MgCl_2$, 150 mM NaCl, and 5 mM β-mercaptoethanol. (C, D) Effect of 8 M urea on complex stability at different pH conditions. The experimental conditions were as described in panels A and B. All buffers were supplemented with 8 M urea. The samples were equilibrated for 12 h at 20 °C. (E) Effect of increasing urea concentration on stalk complexes, monitored as changes of fluorescence intensity at 350 nm at 20 °C, pH 7.5.

from the TH230 trimer at much lower accelerating voltages (20−40 V) than from the stalk pentamer TH199 (80−100 V), indicating that TH199 is more stable than TH230 in the gas phase (Figure 4, charge states in the range 3+ to 7+, marked by red points). Additionally, in-source collision-induced dissociation of the stalk pentamer TH199 and trimer TH230 was carried out by stepwise increasing the cone voltage from 80 to 140 V (Supporting Information, Figure S1). As before, at a low value (80 V) both complexes were stable in the gas phase (observed as series of peaks with charge states: TH199 14+ to 16+; TH230 10+ to 12+). The signals of individual dissociated P proteins in the spectra of the TH230 trimer appeared at a lower voltage than those in the spectra of the TH199 pentamer, once again underscoring the fact that the P proteins are more readily released from the trimer than from the pentamer. Moreover, at the cone voltage of 140 V the stalk trimer was completely disrupted as there were no peaks for the trimer present in the spectrum, while a significant fraction of the stalk pentamer remained intact. This further supports the conclusion that the TH199 pentamer is more stable than the TH230 trimer. In-solution disruption of the complexes was performed by adding increasing amounts of ethanol (EtOH) (Figure 5) or dimethyl sulfoxide (DMSO) (Supporting Information, Figure S2). These organic solvents perturb hydrophobic interactions between proteins. MS analysis revealed that individual P proteins were released more easily in such conditions, indicating that hydrophobic forces play an important role in complex stabilization; especially it was seen in the case of the TH230 trimer.

The main advantage of the nondenaturing mass spectrometry analysis is the ability to progressively disassemble oligomeric complexes, which allows identifying intermediate complex species of possible functional relevance. Thus, upon changing the experimental parameters, not only we were able to disrupt the stalk complexes but, more importantly, the complexes were

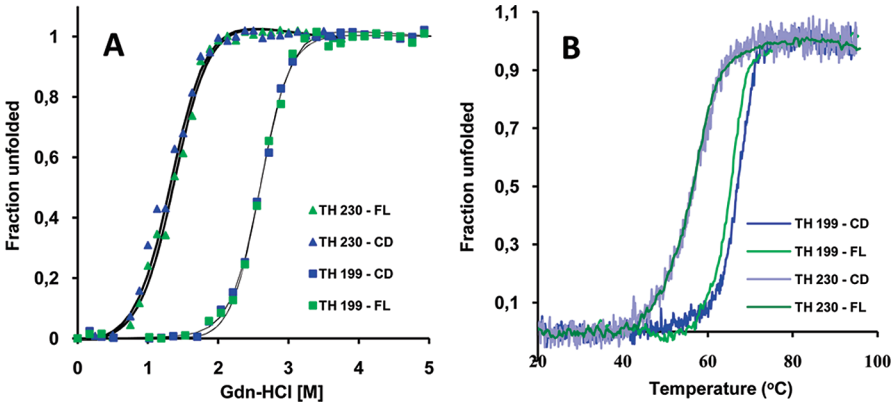

FIGURE 3: Equilibrium unfolding of TH199 and TH230 complexes. Normalized denaturation curves of stalk complexes. (A) Chemical unfolding as a function of Gdn-HCl concentration; fluorescence was monitored at 350 nm and ellipticity at 222 nm, shown. (B) Thermal denaturation; data were fitted to a two-state van't Hoff equation using the PeakFit program. CD and FL means circular dichroism and fluorescence analyses, respectively.

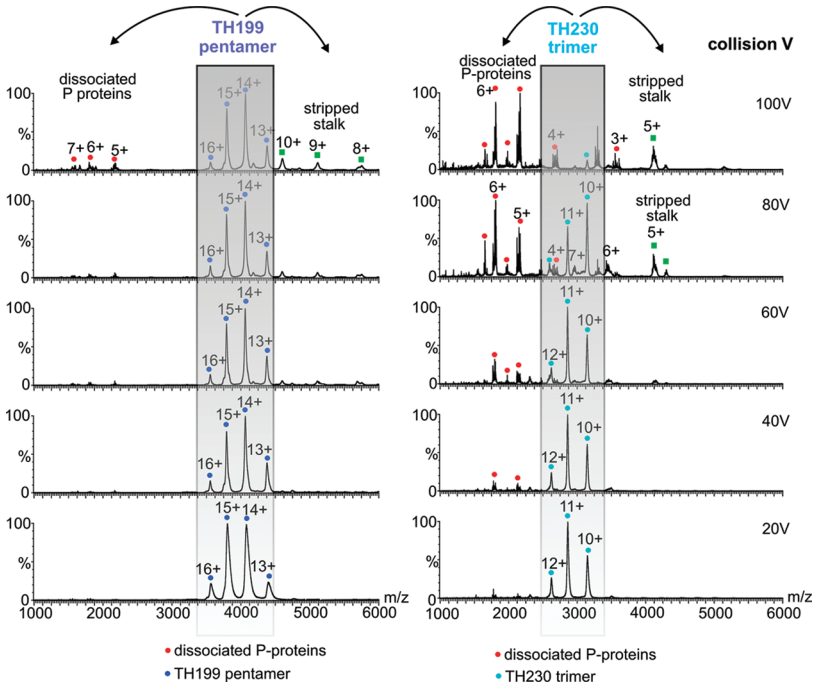

FIGURE 4: Nondenaturing mass spectrometry analysis of TH199 and TH230 complexes. Stalk pentamer TH199 and trimer TH230 were analyzed at different collision energies as indicated on the right (20−100 V). The spectrum shows release of individual P proteins from stalk complexes and formation of stripped complexes, as indicated by arrows. Positions of peaks which correspond to intact complexes are marked with a gray box and blue and magenta spots. Positions of dissociated P proteins are indicated by red dots (P proteins include P1/P2 and P0 deletion form). Peaks corresponding to stripped complexes are marked with green squares. Numbers above peaks indicate charge states of individual complexes/proteins.

disrupted gradually, revealing relationships among the proteins within the stalk complex. As shown in Figure 4, mass spectra of the stalk complexes subjected to the accelerating voltage of 100 V in the collision cell are of particular interest (Figure 4, panel 100 V). At this particular condition, apart from the intact complexes and individual dissociated P proteins, additional complexes appeared, which were named "stripped complexes", whose molecular mass corresponded to the stalk with one or two P proteins removed. However, at 100 V, the stripped complexes were not very well populated. Increasing the collision voltage further (Figure 6, 160 V) made these intermediate species more abundant. As shown in Figure 6, at the accelerating voltage of 160 V the yeast ribosomal stalk TH199 (Figure 6A, charge states 13+ to 17+, blue dots) dissociates into individual P proteins giving rise to a series of 5+ to 7+ charge states at m/z 1500−2300 (Figure 6) and to a number of "stripped complexes" at a higher m/z region. Analysis of the mass spectra of the intermediate species shows two predominant "stripped complexes" of molecular masses 45854 and 35250 Da. These complexes were assigned to TH199 without P2A and without P1B and P2A, respectively. The percentage of the stalk pentamer measured mass increase due to adducts versus the theoretical calculated mass of the stalk pentamer and those for the "stripped complexes" in the same spectrum strongly indicates that the 45854 Da species corresponds to the pentamer lacking P2A and the 35250 Da species to the pentamer devoid of the P1B and P2A proteins. Similar "stripped complexes" were also observed in the case of the TH230 trimer (Figure 4, TH230). The masses of the complexes correspond to heterodimers $\Delta P0_{230-312}$ with either P2A or P1B (Table 2), showing that the P0 protein may independently bind

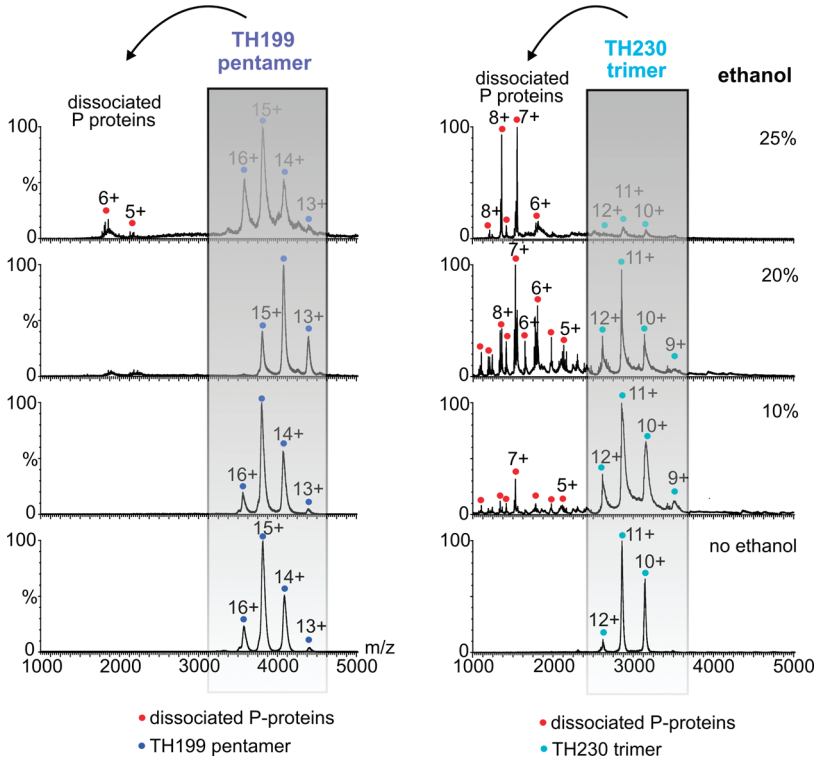

FIGURE 5: Gas phase stability of TH199 and TH230 complexes in the presence of EtOH. Effect of increasing concentration of EtOH, as indicated on the right, was analyzed by mass spectrometry. The mass spectrum was acquired at a cone voltage of 80 V. It shows release of individual P proteins from stalk complexes upon EtOH treatment, as indicated by arrows. For more details see description of Figure 4.

Table 2: Masses of Protein Species Detected by Mass Spectrometry[a]

protein/complex	calcd mass	measured mass	inferred modifications
TH199 pentamer*	56515	56763.58 ± 20.47	
pentamer*, minus P2A	45769	45853.64 ± 25.79	
pentamer*, minus P2A and P1B	35085	35249.63 ± 10.90	
$P0_{199}$	13127	not observed	
$P0_{199}/P_i$	13207	13212.39 ± 0.64	P_i
$P0_{199}/2P_i$	13287	13286.01 ± 9.89	$2P_i$
P1A	10908	10901.73 ± 0.7	
P1B	10668	not observed	
P1B, minus Met, N-acetylation	10 579	10582.60 ± 1.71	minus Met, N-acetylation
P1B, minus Met N-acetylation/P_i	10 659	10662.22 ± 0.7	P_i
P2A	10746	10747.84 ± 1.41	
P2A/P_i	10826	10828.30 ± 0.74	P_i
P2B	11050	11052.80 ± 0.85	
P2B/P_i	11130	11132.95 ± 1.15	P_i
TH230 trimer*	31223.5	31393.69 ± 17.06	
$P0_{230}$	9809.5	9814.23 ± 0.32	
$P0_{230}/P_i$	9889.5	9893.11 ± 0.62	P_i
$P0_{230}$* + P2A	20555.5	20719.08 ± 7.48	
$P0_{230}$* + P1B	20477.5	20565.54 ± 9.21	

[a]Masses of complexes are provided without indication of posttranslational modifications due to heterogeneous population of analyzed protein complexes*.

the P1B and P2A proteins and therefore might play a scaffolding role for the latter.

Mass spectrometry may also be used to study posttranslational modification in a systematic manner. The P proteins are phosphorylated (*34*), and additionally some of them undergo further modifications, but no comprehensive studies of the whole stalk complex have been undertaken until now. We studied the mass spectra of the wild-type stalk isolated from logarithmically growing yeast culture, i.e., from the phase of growth when the highest protein synthesis rate is to be expected. As shown in Figure 6B, expansion of the low *m*/*z* region of the spectrum shows the mass spectra of individual ribosomal stalk proteins P1A, P1B, P2A, and P2B and reveals three series of peaks, P1B/P_i, P2A/P_i, and P2B/P_i, assigned to phosphorylated forms of the respective P proteins, which in fact are the dominant forms in the analyzed spectra. However, the measured molecular mass of P1B (10582.60 ± 1.71 Da) is slightly lower than the calculated theoretical mass (10668), most likely indicating posttranslational modification corresponding to the removal of the first methionine and N-terminal acetylation, which is consistent with earlier data (*35*). This N-terminally modified form of P1B is also phosphorylated. Interestingly, there are no peaks corresponding

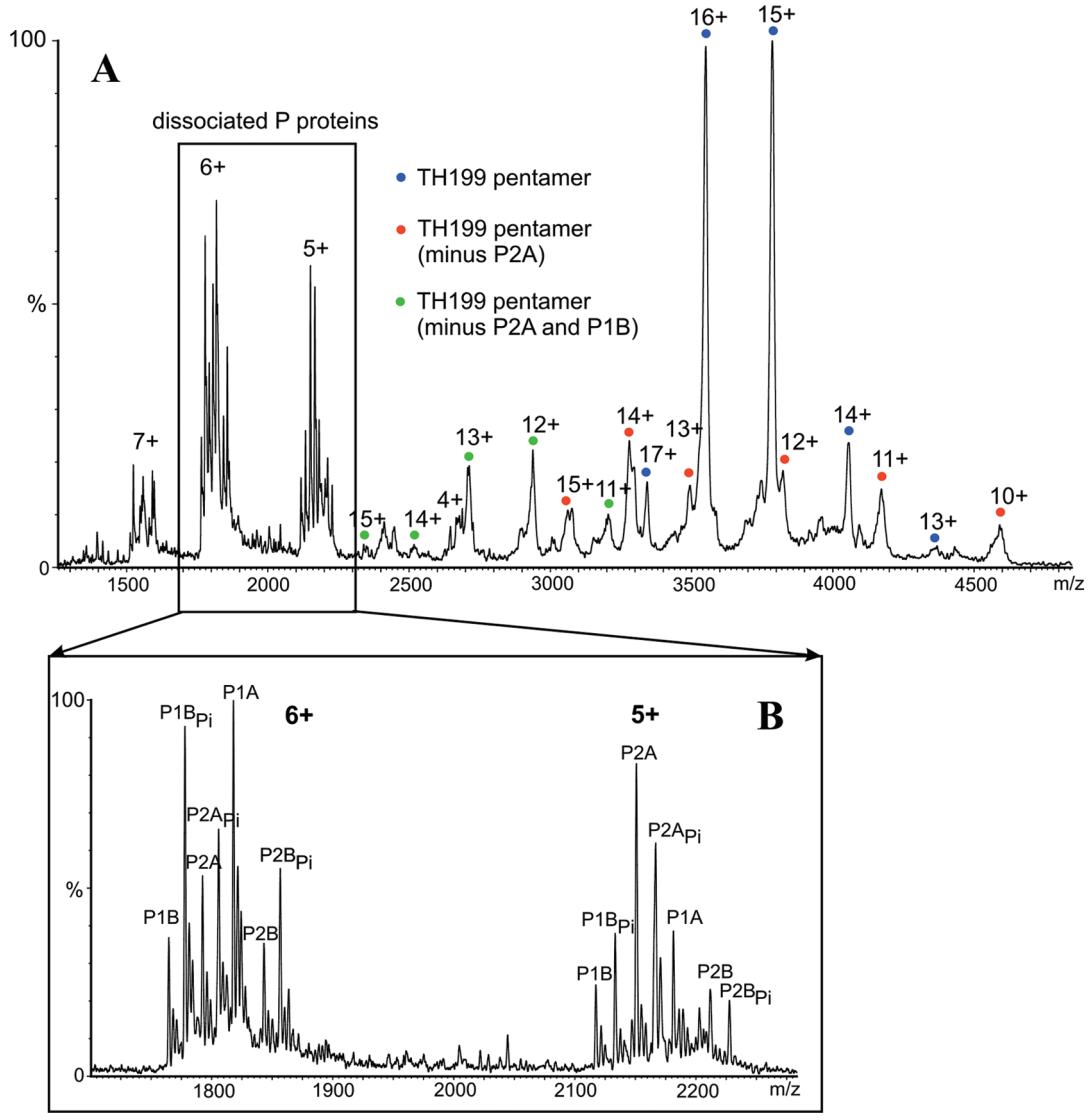

FIGURE 6: Top-down mass spectrometry analysis of the TH199 stalk pentamer. (A) Mass spectrum of TH199 acquired at a collision voltage of 160 V; individual protein species are marked by dots: blue, whole pentamer; red and green, pentamer lacking P2A and P2A/P1B proteins, respectively. Dissociated P proteins are marked with a box. (B) Expansion of low m/z region of spectrum from panel A, $m/z \sim 2000$, showing peaks assigned to dissociated individual P1 and P2 proteins; P_i indicates phosphorylated forms of P proteins.

to a phosphorylated form of P1A in the spectrum (Figure 6B) and no sign of N-terminal acetylation of this protein. Additionally, the N-terminally truncated P0 mutant proteins were also examined, and for both P0 fragments ($\Delta P0_{199-312}$ and $\Delta P0_{230-312}$) two forms were found, a nonphosphorylated and a phosphorylated one, with $\Delta P0_{199-312}$ possibly having two phosphate groups (summarized in Table 2).

DISCUSSION

The eukaryotic ribosomal stalk, although a crucial element of the ribosome, and generally accepted to play important roles in all steps of protein synthesis, is still poorly understood functionally and structurally. In particular, the structural aspects of the stalk as a whole, such as its assembly mode and the function of the individual components in structure formation, have not been studied in detail. On the basis of the available data the stalk is seen as an ensemble of two P1-P2 dimers, in yeast P1A-P2B and P1B-P2A, anchored to the P0 protein. It has been shown that the assembly of the stalk in solution seems to be driven by the P1A-P2B dimer, while the P1B/P2A proteins are probably not directly involved in the P0 folding (*28*). However, all of those data were gained based on *in vitro* assembled incomplete stalk complexes; thus the picture of the formation of the stalk is fragmentary at best, and its relevance to the native structure has yet to be shown. To extend those studies, we have designed a genetically modified yeast system to obtain a natively assembled stalk, where the P protein complex is specifically released from the ribosome using site-specific thrombin cleavage (*19*). Having such natively assembled stalk in its two structural forms (pentameric and trimeric), here we have addressed three aspects of the biological properties of the complex: stability, assembling, and posttranslational modifications. The first remarkable information about the two complexes was provided by biophysical analyses, where the fluorescence analysis showed that the pentamer had a blue-shifted maximum, typical for protein complexes with tryptophan residues fully buried in a hydrophobic protein core, the fact never observed for individual P1-P2 heterodimers. On the other hand, the trimeric complex lacking the P1A-P2B dimer had a red-shifted fluorescence maximum close to 350 nm, indicating that the only tryptophan residue present in the P1B protein is highly exposed to the solvent and demonstrating at the same time that

the complex is rather loosely packed. A similar behavior was observed before for the individual P1-P2 dimer, where the fluorescence maximum of the tryptophan residue was also red shifted (*20*, *36*). Thus, the two complexes studied here exhibited quite different fluorescence spectra, indicating that the pentamer is fully folded, with the two tryptophan residues residing within a stable hydrophobic core. This was supported by experiments in which urea was used as a denaturant. The pentamer was stable in the whole range of urea concentrations, unlike the trimer which exhibited cooperative unfolding that could be fitted into a two-state model. It seems that this remarkable behavior of the eukaryotic stalk pentamer represents a similar feature to the bacterial stalk in *E. coli*, because the bacterial analogue is also resistant to 8 M urea and was characterized before as the L8 complex (*37*). However, considering the stability of the *E. coli* and yeast complexes, there are some differences between them; for example, *E. coli* pentamer L10-$(L7/L12)_2$ can be released intact from the ribosome by ethanol/NH_4Cl treatment (*38*), while in the case of yeast, only P1/P2 proteins are detached from the ribosome, and P0 remain on the ribosome (*39*). These distinct properties can probably be attributed to differences in the rRNA-binding domains of the L10/P0 proteins, and the release of P proteins by ethanol is probably related to their higher sensitivity to this reagent, as was observed in our mass spectrometry analysis (discussed elsewhere), where the P1/P2 proteins were easily detached by ethanol. Nevertheless, despite these differences and a lack of apparent evolutionary relationships, the two types of stalk are generally of similar biophysical properties, which probably allow them to perform the same biological function on the ribosome.

Further information about the biophysical properties of the analyzed complexes was obtained from the analysis of their stability profiles using guanidine hydrochloride and thermal unfolding. Despite the multiprotein character of TH199 and TH230 complexes a simple two-state reversible transition equation could be used to fit the experimental data points, suggesting a simple mechanism of TH199 and TH230 folding/assembly. The two-state model was observed following either coincidence of normalized fluorescence (tertiary structure alterations) or ellipticity (secondary structure unfolding) signals (Figure 3). It suggests that folding and assembly are coupled processes, and the stalk constitutes integrated structure. This idea is supported also by the energetic profiles of the complexes; one finds that the free energy changes of the trimer resemble those found for the P1A-P2B dimer (*20*, *36*) and are more than two times lower than those for the pentamer, once again underscoring the high structural stability of the whole stalk. Taken together, the spectroscopic data demonstrate that the stalk as a whole is a very stable entity, in which the cooperative interactions between all P1/P2 proteins contribute to this high stability. But, when the P1A-P2B dimer is absent, a significant decrease of the stability is observed, showing that this dimer may constitute an important consolidation factor. This concept is in accordance with our previous report, where this dimer was shown to guide proper folding of the P0 protein, which could not be achieved by the P1B/P2A proteins (*28*).

To cast more light on the interplay among the P proteins within the stalk structure, we have applied nondenaturing mass spectrometry analysis, an approach beyond classical biophysical analyses, which allowed an insight into the stalk structure topology from a different angle. The structural properties of the complexes inferred from the fluorescence and CD analyses are fully supported by the mass spectrometry analysis; the pentamer was by far more stable than its depleted form, the trimeric complex. But mass spectrometry analysis allowed us to examine not only the overall stability of the complexes but also the structural relationships among the stalk components. We applied varying mass spectrometry conditions to disrupt the stalk complexes in the gas phase and to focus on different structural components of the stalk complex. The analyses produced three types of spectra. In the gentle ionization conditions we observed only the predominant spectrum specific for the whole stalk, but on increasing the harshness of conditions two other spectra appeared, derivatives of the main one. The second spectrum, very well populated, corresponded to the individual P1/P2 and P0 proteins. The third spectrum, a minor one, was assigned to intermediate complex species, the "stripped complexes". The appearance of the stripped complexes in the mass spectra allowed an insight into the mode of dissembling/assembling of the stalk. By analyzing the molecular masses of the intermediate species, we concluded that the pentameric complex formed two stripped complexes, $\Delta P0_{199-312}$-(P1A-P2B)-(P1B) and $\Delta P0_{199-312}$-(P1A-P2B); thus P2A must have been the first component to leave the complex, and then P1B could be detached, which suggested a sequential depletion: P2A leaving the complex first, followed by P1B. There was no sign of the other stripped complexes, missing the P1A and/or P2B proteins. This shows that only the P1B−P2A dimer can leave the pentameric complex, probably in a sequential manner. In the case of the analyzed trimer, two types of stripped complexes were detected: dimers $\Delta P0_{230-312}$-(P2A) and $\Delta P0_{230-312}$-(P1B). The existence of these two stable dimers indicates that P0 protein contains two independent binding sites for the P1B and P2A. It seems that formation of a stable P1B-P2A dimer is dependent on the presence of the P0, and therefore P0 may act as a scaffolding protein for the P1B and P2A proteins. This idea is in accordance with our previous observation (*28*), where we showed that P1B and P2A proteins could interact with P0 independently but could not efficiently form the heterodimer in solution (*40*). This observation is further supported by an *in vivo* analysis which suggested that the stalk could undergo changes in protein composition with respect to the P1B/P2A as a very dynamic system, where the P2A protein is the most active part (*41*). Our present data offer the first structural proof that the exchangeability of the P proteins may indeed take place as proposed before (*42*, *43*), showing that only the P1B/P2A proteins have the capacity to leave the ribosomal particle. The P1A/P2B proteins showed a different behavior. We have not been able to observe stripped complexes deprived of P2B and/or P1A in the mass spectra regardless of the methods used, indicating high stability/integrity of the P0-(P1A-P2B) complex. Taking into account the present biophysical data and nondenaturing mass spectrometry analyses, and our previous folding experiments (*40*) and biophysical analyses of P protein dimers (*20*, *36*), a coherent view about the assembling of the yeast stalk is emerging (Figure 7). The P1A-P2B dimer together with the P0 protein is the core structural element which ensures structural stability of the stalk, and probably trimer P0-(P1A-P2B) is assembled first where the P1A-P2B dimer acts as a chaperone-like factor facilitating P0 folding, and therefore assembling and folding are coupled processes. On the other hand, formation of the P1B/P2A dimer is dependent on P0 and these proteins likely represent a dynamic regulatory element(s), and as suggested before is probably protein synthesis dependent (*44*). Our study is a

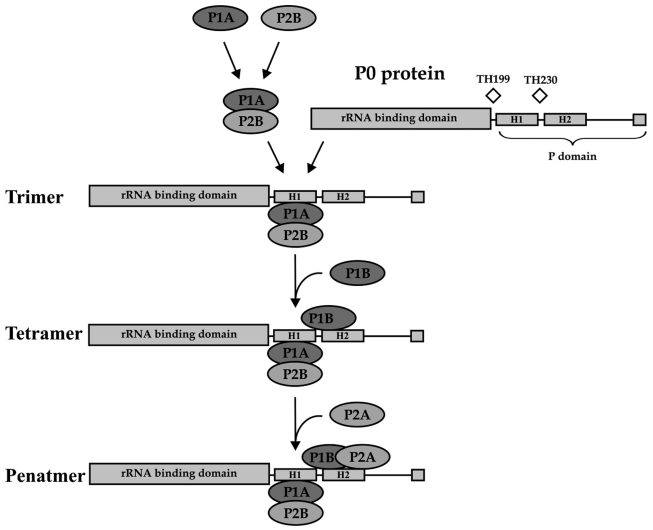

FIGURE 7: Scheme for the pathway of stalk assembling. P1A and P2B proteins form dimer independently of other stalk components, and the dimer may act as a chaperone-like factor facilitating proper P0 folding. The trimeric complex P0-(P1A-P2B) operates as a scaffolding factor for two other P-proteins, with P1B attaching to the complex first, followed by P2A. There are two autonomous binding sites, H1 and H2, for two protein dimers (*19*); however, P1B and P2A proteins are able to interact with P0 independently. The rRNA and P domains are indicated; diamonds show cleavage sites for thrombin present in P0 at position 199 or 230.

significant extension of the pioneering work on the stalk assembly in which a top-down proteomic approach was applied for analysis of intact yeast ribosomal particles (*45*). Those authors have shown that the extent to which individual proteins are released in tandem mass spectrometry is related to their location in the complex, such that the intensity of peaks assigned to the P2 proteins is greater than for the P1 proteins. Evidence was provided that the full complement of the P proteins is required for the stalk complex stability. However, they failed to provide a clear view on the stalk assembly, leaving the problem open, because of the extensive overlap of the peaks and the overall complexity of the spectra. By using isolated native stalk complexes, a much less complex system, we could unequivocally assign all of the peaks, providing clear-cut data.

Having determined the relative stability of the isolated stalk complexes, we have also analyzed posttranslational modifications of all P proteins in the logarithmic phase of yeast growth. It was already known that P proteins are phosphorylated (*34*) and additionally P1 proteins are acetylated (*35*). However, those data came from scattered studies and have never been collected from a single analysis reflecting particular biological state. Our method of *in vivo* stalk preparation allowed isolation of the whole stalk from a single point of yeast growth (logarithmic phase). Monophosphorylation of P proteins was the prevalent modification, except for the P1A protein which was not phosphorylated. Interestingly, the $\Delta P0_{199-312}$ protein was detected in a diphospho form, which has not been observed for P0. Additionally, P1B was confirmed to be acetylated (*35*), but P1A is not, contrary to an earlier report (*35*). This variability regarding P1A acetylation resembles the behavior of analogous *E. coli* L7 and L12 proteins which undergo differential acetylation during growth and might be attributed to the cell's strategy to increase the stability of the stalk complex under stress conditions (*46*). This similarity is yet another common functional characteristic of the bacterial and eukaryal stalk. These findings show the very complex nature of the yeast stalk, underscoring the view that this structure might be involved in the complicated regulation of eukaryotic gene expression on the translational level.

SUPPORTING INFORMATION AVAILABLE

Figure S1, spectra of stalk pentamer TH199 and trimer TH230 acquired at different cone voltages, and Figure S2, gas phase stability of TH199 and TH230 complexes in the presence of DMSO. This material is available free of charge via the Internet at http://pubs.acs.org.

REFERENCES

1. Liljas, A. (2004) Structural Aspects of Protein Synthesis, World Scientific Publishing, Singapore.
2. Gomez-Lorenzo, M. G., Spahn, C. M., Agrawal, R. K., Grassucci, R. A., Penczek, P., Chakraburtty, K., Ballesta, J. P., Lavandera, J. L., Garcia-Bustos, J. F., and Frank, J. (2000) Three-dimensional cryo-electron microscopy localization of EF2 in the *Saccharomyces cerevisiae* 80S ribosome at 17.5 Å resolution. *EMBO J. 19*, 2710–2718.
3. Diaconu, M., Kothe, U., Schlunzen, F., Fischer, N., Harms, J. M., Tonevitsky, A. G., Stark, H., Rodnina, M. V., and Wahl, M. C. (2005) Structural basis for the function of the ribosomal L7/12 stalk in factor binding and GTPase activation. *Cell 121*, 991–1004.
4. Wahl, M. C., and Moller, W. (2002) Structure and function of the acidic ribosomal stalk proteins. *Curr. Protein Pept. Sci. 3*, 93–106.
5. Gonzalo, P., and Reboud, J. P. (2003) The puzzling lateral flexible stalk of the ribosome. *Biol. Cell 95*, 179–193.
6. Ballesta, J. P., and Remacha, M. (1996) The large ribosomal subunit stalk as a regulatory element of the eukaryotic translational machinery. *Prog. Nucleic Acid Res. Mol. Biol. 55*, 157–193.
7. Brodersen, D. E., and Nissen, P. (2005) The social life of ribosomal proteins. *FEBS J. 272*, 2098–2108.
8. Wimberly, B. T., Guymon, R., McCutcheon, J. P., White, S. W., and Ramakrishnan, V. (1999) A detailed view of a ribosomal active site: the structure of the L11-RNA complex. *Cell 97*, 491–502.
9. Kavran, J. M., and Steitz, T. A. (2007) Structure of the base of the L7/L12 stalk of the *Haloarcula marismortui* large ribosomal subunit: analysis of L11 movements. *J. Mol. Biol. 371*, 1047–1059.
10. Ilag, L. L., Videler, H., McKay, A. R., Sobott, F., Fucini, P., Nierhaus, K. H., and Robinson, C. V. (2005) Heptameric (L12)6/L10 rather than canonical pentameric complexes are found by tandem MS of intact ribosomes from thermophilic bacteria. *Proc. Natl. Acad. Sci. U.S.A. 102*, 8192–8197.
11. Maki, Y., Hashimoto, T., Zhou, M., Naganuma, T., Ohta, J., Nomura, T., Robinson, C. V., and Uchiumi, T. (2007) Three binding sites for stalk protein dimers are generally present in ribosomes from archaeal organism. *J. Biol. Chem. 282*, 32827–32833.
12. Guarinos, E., Santos, C., Sanchez, A., Qiu, D. Y., Remacha, M., and Ballesta, J. P. (2003) Tag-mediated fractionation of yeast ribosome populations proves the monomeric organization of the eukaryotic ribosomal stalk structure. *Mol. Microbiol. 50*, 703–712.
13. Uchiumi, T., Hori, K., Nomura, T., and Hachimori, A. (1999) Replacement of L7/L12.L10 protein complex in *Escherichia coli* ribosomes with the eukaryotic counterpart changes the specificity of elongation factor binding. *J. Biol. Chem. 274*, 27578–27582.
14. Shimmin, L. C., Ramirez, C., Matheson, A. T., and Dennis, P. P. (1989) Sequence alignment and evolutionary comparison of the L10 equivalent and L12 equivalent ribosomal proteins from archaebacteria, eubacteria, and eucaryotes. *J. Mol. Evol. 29*, 448–462.
15. Lalioti, V. S., Perez-Fernandez, J., Remacha, M., and Ballesta, J. P. (2002) Characterization of interaction sites in the *Saccharomyces cerevisiae* ribosomal stalk components. *Mol. Microbiol. 46*, 719–729.
16. Grela, P., Bernado, P., Svergun, D., Kwiatowski, J., Abramczyk, D., Grankowski, N., and Tchorzewski, M. (2008) Structural relationships among the ribosomal stalk proteins from the three domains of life. *J. Mol. Evol. 67*, 154–167.
17. Remacha, M., Jimenez-Diaz, A., Bermejo, B., Rodriguez-Gabriel, M. A., Guarinos, E., and Ballesta, J. P. (1995) Ribosomal acidic phosphoproteins P1 and P2 are not required for cell viability but regulate the pattern of protein expression in *Saccharomyces cerevisiae*. *Mol. Cell. Biol. 15*, 4754–4762.
18. Santos, C., and Ballesta, J. P. (1995) The highly conserved protein P0 carboxyl end is essential for ribosome activity only in the absence of proteins P1 and P2. *J. Biol. Chem. 270*, 20608–20614.

19. Krokowski, D., Boguszewska, A., Abramczyk, D., Liljas, A., Tchorzewski, M., and Grankowski, N. (2006) Yeast ribosomal P0 protein has two separate binding sites for P1/P2 proteins. *Mol. Microbiol. 60*, 386–400.
20. Tchorzewski, M., Krokowski, D., Boguszewska, A., Liljas, A., and Grankowski, N. (2003) Structural characterization of yeast acidic ribosomal P proteins forming the P1A-P2B heterocomplex. *Biochemistry 42*, 3399–3408.
21. Tchorzewski, M., Boldyreff, B., Issinger, O., and Grankowski, N. (2000) Analysis of the protein-protein interactions between the human acidic ribosomal P-proteins: evaluation by the two hybrid system. *Int. J. Biochem. Cell Biol. 32*, 737–746.
22. Gonzalo, P., Lavergne, J. P., and Reboud, J. P. (2001) Pivotal role of the P1 N-terminal domain in the assembly of the mammalian ribosomal stalk and in the proteosynthetic activity. *J. Biol. Chem. 276*, 19762–19769.
23. Zurdo, J., Parada, P., van den Berg, A., Nusspaumer, G., Jimenez-Diaz, A., Remacha, M., and Ballesta, J. P. (2000) Assembly of *Saccharomyces cerevisiae* ribosomal stalk: binding of P1 proteins is required for the interaction of P2 proteins. *Biochemistry 39*, 8929–8934.
24. Shimizu, T., Nakagaki, M., Nishi, Y., Kobayashi, Y., Hachimori, A., and Uchiumi, T. (2002) Interaction among silkworm ribosomal proteins P1, P2 and P0 required for functional protein binding to the GTPase-associated domain of 28S rRNA. *Nucleic Acids Res. 30*, 2620–2627.
25. Guarinos, E., Remacha, M., and Ballesta, J. P. (2001) Asymmetric interactions between the acidic P1 and P2 proteins in the *Saccharomyces cerevisiae* ribosomal stalk. *J. Biol. Chem. 276*, 32474–32479.
26. Zurdo, J., Gonzalez, C., Sanz, J. M., Rico, M., Remacha, M., and Ballesta, J. P. (2000) Structural differences between *Saccharomyces cerevisiae* ribosomal stalk proteins P1 and P2 support their functional diversity. *Biochemistry 39*, 8935–8943.
27. Hagiya, A., Naganuma, T., Maki, Y., Ohta, J., Tohkairin, Y., Shimizu, T., Nomura, T., Hachimori, A., and Uchiumi, T. (2005) A mode of assembly of P0, P1, and P2 proteins at the GTPase-associated center in animal ribosome: in vitro analyses with P0 truncation mutants. *J. Biol. Chem. 280*, 39193–39199.
28. Krokowski, D., Tchorzewski, M., Boguszewska, A., and Grankowski, N. (2005) Acquisition of a stable structure by yeast ribosomal P0 protein requires binding of P1A-P2B complex: in vitro formation of the stalk structure. *Biochim. Biophys. Acta 1724*, 59–70.
29. Gill, S. C., and von Hippel, P. H. (1989) Calculation of protein extinction coefficients from amino acid sequence data. *Anal. Biochem. 182*, 319–326.
30. Santoro, M. M., and Bolen, D. W. (1992) A test of the linear extrapolation of unfolding free energy changes over an extended denaturant concentration range. *Biochemistry 31*, 4901–4907.
31. Sobott, F., Hernandez, H., McCammon, M. G., Tito, M. A., and Robinson, C. V. (2002) A tandem mass spectrometer for improved transmission and analysis of large macromolecular assemblies. *Anal. Chem. 74*, 1402–1407.
32. Sharon, M., and Robinson, C. V. (2007) The role of mass spectrometry in structure elucidation of dynamic protein complexes. *Annu. Rev. Biochem. 76*, 167–193.
33. Robinson, C. V., Sali, A., and Baumeister, W. (2007) The molecular sociology of the cell. *Nature 450*, 973–982.
34. Zambrano, R., Briones, E., Remacha, M., and Ballesta, J. P. (1997) Phosphorylation of the acidic ribosomal P proteins in *Saccharomyces cerevisiae*: a reappraisal. *Biochemistry 36*, 14439–14446.
35. Santos, C., Ortiz-Reyes, B., Naranda, T., Remacha, M., and Ballesta, J. P. (1993) The acidic phosphoproteins from *Saccharomyces cerevisiae* ribosomes. NH_2-terminal acetylation is a conserved difference between P1 and P2 proteins. *Biochemistry 32*, 4231–4236.
36. Grela, P., Sawa-Makarska, J., Gordiyenko, Y., Robinson, C. V., Grankowski, N., and Tchorzewski, M. (2008) Structural properties of the human acidic ribosomal P proteins forming the P1-P2 heterocomplex. *J. Biochem. 143*, 169–177.
37. Pettersson, I., Hardy, S. J., and Liljas, A. (1976) The ribosomal protein L8 is a complex L7/L12 and L10. *FEBS Lett. 64*, 135–138.
38. Highland, J. H., and Howard, G. A. (1975) Assembly of ribosomal proteins L7, L10, L11, and L12, on the 50 S subunit of *Escherichia coli*. *J. Biol. Chem. 250*, 813–814.
39. Towbin, H., Ramjoue, H. P., Kuster, H., Liverani, D., and Gordon, J. (1982) Monoclonal antibodies against eucaryotic ribosomes. Use to characterize a ribosomal protein not previously identified and antigenically related to the acidic phosphoproteins P1/P2. *J. Biol. Chem. 257*, 12709–12715.
40. Tchorzewski, M., Boguszewska, A., Dukowski, P., and Grankowski, N. (2000) Oligomerization properties of the acidic ribosomal P-proteins from *Saccharomyces cerevisiae*: effect of P1A protein phosphorylation on the formation of the P1A-P2B hetero-complex. *Biochim. Biophys. Acta 1499*, 63–73.
41. Garcia-Marcos, A., Sanchez, S. A., Parada, P., Eid, J., Jameson, D. M., Remacha, M., Gratton, E., and Ballesta, J. P. (2008) Yeast ribosomal stalk heterogeneity in vivo shown by two-photon FCS and molecular brightness analysis. *Biophys. J. 94*, 2884–2890.
42. Tsurugi, K., and Ogata, K. (1985) Evidence for the exchangeability of acidic ribosomal proteins on cytoplasmic ribosomes in regenerating rat liver. *J. Biochem.* (*Tokyo*) *98*, 1427–1431.
43. Zinker, S., and Warner, J. R. (1976) The ribosomal proteins of *Saccharomyces cerevisiae*. Phosphorylated and exchangeable proteins. *J. Biol. Chem. 251*, 1799–1807.
44. Remacha, M., Jimenez-Diaz, A., Santos, C., Briones, E., Zambrano, R., Rodriguez Gabriel, M. A., Guarinos, E., and Ballesta, J. P. (1995) Proteins P1, P2, and P0, components of the eukaryotic ribosome stalk. New structural and functional aspects. *Biochem. Cell Biol. 73*, 959–968.
45. Hanson, C. L., Videler, H., Santos, C., Ballesta, J. P., and Robinson, C. V. (2004) Mass spectrometry of ribosomes from *Saccharomyces cerevisiae*: implications for assembly of the stalk complex. *J. Biol. Chem. 279*, 42750–42757.
46. Gordiyenko, Y., Deroo, S., Zhou, M., Videler, H., and Robinson, C. V. (2008) Acetylation of L12 increases interactions in the *Escherichia coli* ribosomal stalk complex. *J. Mol. Biol. 380*, 404–414.